ELSEVIER

Journal of Organometallic Chemistry 555 (1998) 177–185

Journal of Organometallic Chemistry

New O- and N-bonded zirconocene complexes and their catalytic properties in ethylene polymerization. X-ray crystal structure of $(C_5H_5)_2Zr\{2,6\text{-}OC_6H_3(CH_3)_2\}_2$, $(C_5H_5)_2Zr\{2,4,6\text{-}OC_6H_2(CH_3)_3\}_2$ and $(C_5H_5)_2Zr(CH_3)\{CH(NC_6H_5)_2\}$

F. Benetollo [a,*], G. Cavinato [b], L. Crosara [b], F. Milani [c], G. Rossetto [a], C. Scelza [a], P. Zanella [a]

[a] *ICTIMA–MITER, CNR, Corso Stati Uniti 4, 35127, Padova, Italy*
[b] *Dipartimento di Chimica Inorganica Metallorganica ed Analitica, Università di Padova, Via Loredan 4, 35100, Padova, Italy*
[c] *Polimeri Europa, P. le Donegani 12, 44100, Ferrara, Italy*

Received 2 August 1997

Abstract

A series of zirconocene complexes of formula $Cp_2ZrMe_{2-n}L_n$ where $Cp = C_5H_5^-$, Me = methyl, L = pyrazolyl, bis(*N*,*N*′-phenylformamidinato), or substituted aryloxide and $n = 1,2$, were synthesized by reaction of Cp_2ZrCl_2 and Cp_2ZrMe_2 with LiL or HL, respectively. The structures of $Cp_2Zr(2,6\text{-}OC_6H_3Me_2)_2$, $Cp_2Zr(2,4,6\text{-}OC_6H_2Me_3)_2$ and $Cp_2ZrMe\{CH(NC_6H_5)_2\}$ were determined by single crystal X-ray diffraction. The complexes demonstrate appreciable activity for ethylene polymerization when used as cocatalysts with methylaluminoxane and dimethylanilinium tetrafluorophenylborate. © 1998 Elsevier Science S.A. All rights reserved.

Keywords: Zirconocene compounds; Synthesis; Ethylene polimerization; Crystal structure

---

1. Introduction

The catalytic activity of zirconocene complexes of the type Y_2ZrL_2 (Y = cyclopentadienyl, indenyl, fluorenyl; L = halide, alkyl etc.) in the polymerization of α-olefins has been the object of both fundamental and applied studies, especially after it was reported that the presence of partially hydrolyzed trimethylaluminum (MAO = methylalumoxane) has a favourable effect on the process [1]. For the prototype catalyst Cp_2ZrMe_2, where $Cp = C_5H_5^-$ and $Me = CH_3$, the fundamental step of the reaction is the interaction of Cp_2ZrMe_2 with MAO, or with other acidic agents such as R_3NHA or BR_3 (R = tetrapentafluorophenylborate) to yield a coordinatively unsaturated cationic species [2–6]. The latter initiates the polymerization by coordination of the olefin double bond to zirconium, and propagates it by insertion of the coordinated olefin into the Zr–Me bond. The resulting polymeric chain, Zr-$(CH_2CH_2)_n$Me, eventually undergoes Zr-(polymer) scission. Thus the overall polymerization process may be schematically represented as follows:

$$Cp_2ZrMe_2 + MAO \rightarrow Cp_2ZrMe^+ + [Me(MAO)]^- \quad (1)$$

$$Cp_2ZrMe^+ + \text{olefin} \rightarrow Cp_2Zr^+ \text{ (olefin) Me} \quad (2)$$

$$Cp_2Zr^+\text{(olefin)Me} + n - 1 \text{ olefin} \rightarrow Cp_2Zr(\text{polymer})^+ \quad (3)$$

The activity of the catalyst, as well as several important properties of the polymer such as molecular weight and molecular weight distribution, are strongly dependent on the electronic and steric features of the ligands bound to the Zr center in the active cationic species.

---

[*] Corresponding author. Tel.: +39 49 8295611; fax: +39 49 8702911.

PII S0022-328X(97)00775-4

Numerous publications and patents have focused on the effects of the π-bonded, cyclopentadienyl, indenyl and fluorenyl ligands, both as such and in variously substituted (eventually bridged) forms; information on the effects of σ-bonded ligands other than CH_3 or Cl are far more limited. It was of interest, therefore, to investigate the catalytic activity of zirconocene complexes of the type $Cp_2ZrMe_{2-n}L_n$ (L = substituted aryloxide, pyrazolyl, *N*,*N'*-diphenylformamidinato; $n = 1,2$), which offer a variety of steric, electronic and bonding features. Mixed ligands and amidinato Zr systems have been recently described by Green and coworkers [7].

2. Results and discussion

Two series of zirconium-biscyclopentadienyl complexes, of general formula Cp_2ZrMeL (L = 2,6-$OC_6H_3Me_2$ **4**, $C_3H_3N_2$ **8** [7,8], $CH(NC_6H_5)_2$ **10**) and Cp_2ZrL_2 (L = OC_6H_5 **3** [7,9], 2,6-$OC_6H_3Me_2$ **5**, 2,4,6-$OC_6H_2Me_3$ **6**, 4-$OC_6H_4{}^tBu$ **7**, $C_3H_3N_2$ **9**, $CH(NC_6H_5)_2$ **11**) were synthesized by reaction of Cp_2ZrCl_2 (**1**) and Cp_2ZrMe_2 (**2**) with the appropriate HL ligand or its lithium salt:

$$Cp_2ZrMe_2 + nHL \rightarrow Cp_2ZrMe_{2-n}L_n + nCH_4 \qquad (4)$$

$$Cp_2ZrCl_2 + 2LiL \rightarrow Cp_2ZrL_2 + 2LiCl \qquad (5)$$

All reactions were carried out using as solvents anhydrous toluene, benzene or diethylether. Complexes **3**, **4** and **10** were prepared by route 4 at room temperature; **5**, **6** and **7** were obtained by the same route in toluene at reflux temperature; **9** and **11** were prepared by route 5. In each case yields were quantitative and the complexes were easily isolated in pure form, as the by products were either methane gas or solid LiCl, completely insoluble in the non-polar solvent medium. The complexes were thermally stable but were sensitive to normal atmospheric conditions, which prevented their characterization by elemental analysis. The position and intensity of the signals in the ^1H NMR spectra, however, provided unambiguous identification; the spectra of compounds **3** and **8** matched closely those previously reported [9,8] while this work was in progress. Four complexes, three of the aryloxide series and one containing the formamidinato ligand, gave well-formed crystals and the structures of **3**, **5**, **6** and **11** were determined by X-ray crystallography and are discussed in a following section. On the basis of the ^1H NMR evidence, it can be concluded that in solution these complexes retain similar structures, with the central zirconium ion surrounded by two cyclopentadienyls and two other ligands in a pseudotetrahedral geometry. In all complexes the Cp and OAr ligands (Ar = phenyl or substituted phenyl) are coordinated in their typical η^5 and η^1 modes, respectively; the pyrazolyl and formamidinato ligands, instead, may exist in a $\eta^2 \rightleftharpoons \eta^1$ equilibrium which accounts for the equivalence of the corresponding protons (Scheme 1).

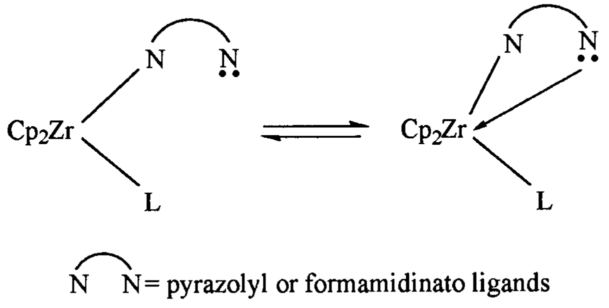

Scheme 1. The pyrazolyl and formamidinato ligands existing in a $\eta^2 \rightleftharpoons \eta^1$ equilibrium.

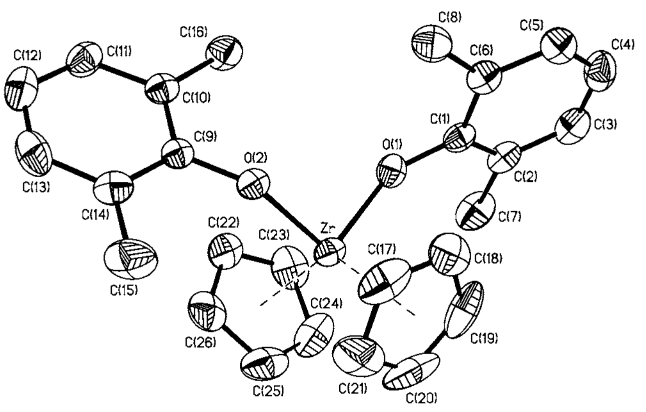

Fig. 1. Molecular structure and atom numbering scheme of $Cp_2Zr(2,6\text{-}OC_6H_3Me_2)_2$.

The mass spectra (MS), of **4** and **5** were consistent with expectations. In **4**, a weak parent peak was observed at *m*/*z* 357 and an intense peak at 342 $(Cp_2ZrOC_6H_3Me_2)^+$ resulted from the easy cleavage of Me. Other fairly intense ions occurred at 276 $(CpZrOC_6H_3MeCH_2)^+$, 229 (Cp_2Zr^+) and 172 $(CpZrO^+)$. The MS spectrum of **5** showed a small peaks at 463 (parent peak, M^+) and 397 (M^+-C_5H_6);

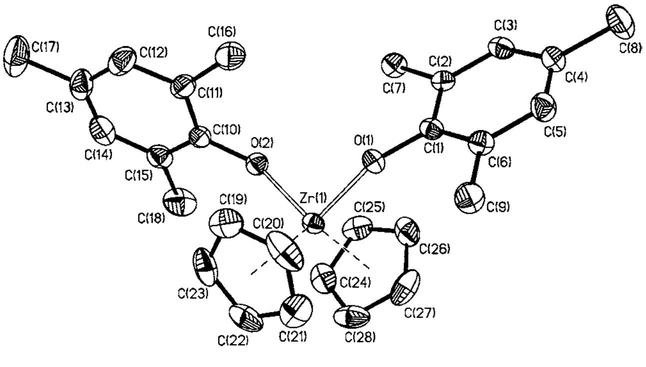

Fig. 2. Molecular structure and atom numbering scheme of $Cp_2Zr(2,4,6\text{-}OC_6H_2Me_3)_2$ (only one of the two independent molecules is shown).

Table 1
Significant bond distances (Å) and angles (°) for the **5** and **6** derivatives

Complexes	**5**	**6**	
Zr–O(1)	1.997(5)	1.996(3)	1.997(4)
Zr–O(2)	1.996(5)	1.989(3)	1.997(4)
Zr–X(1)	2.24(1)	2.249(5)	2.249(8)
Zr–X(2)	2.23(1)	2.252(7)	2.246(6)
X(1)–Zr–X(2)	126.7(4)	126.7(4)	126.6(2)
O(1)–Zr–O(2)	98.6(2)	99.5(1)	98.5(1)
Zr–O(1)–C(1)	145.8(4)	152.6(3)	144.7(3)
Zr–O(2)–C(9)	146.2(5)	145.9(3)	146.9(3)
O(1)–Zr–O(2)–C(9)	103.8(8)	104.1(5)	103.2(5)
O(2)–Zr–O(1)–C(1)	112.5(9)	103.4(6)	102.7(6)

X = centre of the Cp rings.

additional higher intensity peaks identical to those present in **4** probably originated from the species $Cp_2ZrOC_6H_3Me_2^+$.

2.1. Crystal structures of the complexes

The molecular structure of $Cp_2Zr(2,6\text{-}OC_6H_3Me_2)_2$ (**5**) is shown in Fig. 1. The ligands adopt a tetrahedral coordination geometry around the Zr(IV) with the two Cp ligands staggered and the two 2,6-dimethylphenolates in different orientations, as shown by the different values of the two torsion angles C(1)–O(1)–Zr–O(2) (112.5(9)°) and C(9)–O(2)–Zr–O(1) (103.8(8)°). A comparison with the $Cp_2Zr(OC_6H_5)_2$ analog [9] shows that the presence of the two methyl groups in the 2,6-positions of the phenolate rings results in loss of the crystallographic binary symmetry, whereas the bond distances and angles of the Zr(IV) coordination sphere retain comparable values. The same geometric parameters were observed in a new form of the $Cp_2Zr(OC_6H_5)_2$ (**3**)[1] obtained in this work as white prismatic crystals from the reaction mixture. This new form differs from that previously reported [9] by having a O–Zr–O–C torsion angle of 119.4(5)°, instead of 113(1)°.

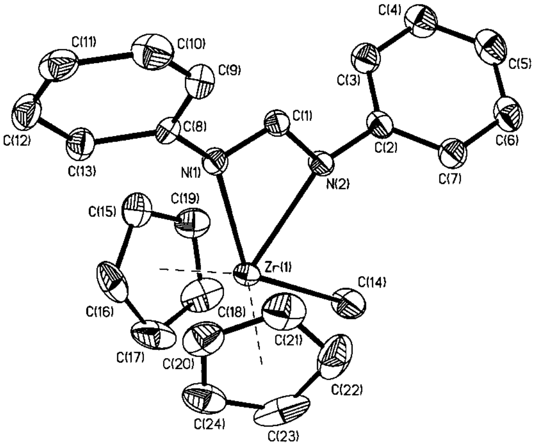

Fig. 3. Molecular structure and atom numbering scheme of $Cp_2ZrMe\{CH(NC_6H_5)_2\}$(only one of the two independent molecules is shown).

Table 2
Selected bond distances (Å) and angles (°) for $Cp_2ZrMe\{CH(NC_6H_5)_2\}$

Molecule **A**		Molecule **B**	
Zr(1)–N(1)	2.367(4)	Zr(2)–N(1A)	2.356(4)
Zr(1)–N(2)	2.324(4)	Zr(2)–N(2A)	2.343(4)
Zr(1)–C(14)	2.314(8)	Zr(1)–C(14A)	2.341(5)
Zr(1)–X(1)	2.238(8)	Zr(2)–X(1A)	2.233(6)
Zr(1)–X(2)	2.241(9)	Zr(2)–X(2A)	2.239(9)
N(1)–C(1)	1.320(8)	N(1A)–C(1A)	1.312(1)
N(1)–C(8)	1.400(7)	N(1A)–C(8A)	1.411(4)
N(2)–C(1)	1.309(6)	N(2A)–C(1A)	1.321(1)
N(2)–C(2)	1.418(7)	N(2A)–C(2A)	1.415(5)
X(1)–Zr(1)–X(2)	129.1(3)	X(1A)–Zr(2)–X(2A)	128.8(3)
C(14)–Zr(1)–X(1)	98.8(4)	C(14A)–Zr(2)–X(1A)	99.5(3)
C(14)–Zr(1)–X(2)	100.3(3)	C(14A)–Zr(2)–X(2A)	109.9(3)
N(1)–Zr(1)–X(1)	99.7(3)	N(1A)–Zr(2)–X(1A)	98.0(2)
N(1)–Zr(1)–X(2)	101.5(3)	N(1A)–Zr(2)–X(2A)	101.3(2)
N(1)–Zr(1)–C(14)	131.9(2)	N(1A)–Zr(2)–C(14A)	132.9(1)
N(1)–Zr(1)–N(2)	56.4(1)	N(1A)–Zr(2)–N(2A)	56.6(1)
N(2)–Zr(1)–X(1)	113.7(2)	N(2A)–Zr(2)–X(1A)	112.1(2)
N(2)–Zr(1)–X(2)	116.6(3)	N(2A)–Zr(2)–X(2A)	118.2(2)
N(2)–Zr(1)–C(14)	75.5(2)	N(2A)–Zr(2)–C(14A)	76.3(2)
C(1)–N(1)–C(8)	122.3(5)	C(1A)–N(1A)–C(8A)	120.0(4)
C(1)–N(2)–C(2)	119.6(4)	C(1A)–N(2A)–C(2A)	118.5(4)
N(1)–C(1)–N(2)	114.9(5)	N(1A)–C(1A)–N(2A)	115.6(4)

X = centre of the Cp rings.

The presence of an additional methyl group in the $Cp_2Zr(2,4,6\text{-}OC_6H_2Me_3)_2$ (**6**) complex (Fig. 2) does not have a major effect on the overall molecular geometry, which shows bond lengths and angles comparable to those of the previously mentioned analogs (see Table 1) The presence of two molecules in the asymmetric unit is justified by the different values of the Zr–O–C angle (152.6(3)° and 145.9(3)° in one molecule, 144.7(3), 146.9(3)° in the other) owing to the facile rotation of the ligand about the O–C bonds. This easy conformational change also explains the existence of two distinct crystal forms for $Cp_2Zr(OC_6H_5)_2$.

The molecular structure of $Cp_2ZrMe\{CH(NC_6H_5)_2\}$ (**11**) (Fig. 3) is characterized by the presence of two molecular conformations in the unit cell, differing chiefly in the mutual orientations of the phenyl rings, which form a dihedral angle of 114° in molecule **A** and of 92° in molecule **B**. Selected geometrical parameters are listed in Table 2 and illustrate the other subtle differences between the two molecules. In molecule **B** the formamidinato ligand, which is coordinated to the metal ion via the two nitrogen atoms, forms a rather

---

[1] Crystal data $-ZrC_{22}H_{20}O_2$, orthorhombic, Pbcn, $a = 17.761(3)$, $b = 11.619(3)$, $c = 21.158(4)$ Å; $V = 1908(1)$ Å^3, $Z = 4$, $Dx = 1.42$ Mg m^{-3}, $\lambda = (\text{MoK}\alpha) = 0.71073$ Å, $T = 293$ K, $R = 0.043$ for 1846 observed reflections.

Table 3
Polymerization results

Catalyst	Yield[a]			M_w	
	t (°C)	BPF_4^b	MAO	BPF_4^b	MAO
Cp_2ZrCl_2 (**1**)	50	1		11 300	
	90	36	68	58 000	20 000
Cp_2ZrMe_2 (**2**)	50	3		25 000	
	90	40	160	55 000	38 500
$Cp_2Zr(OAr)_2$ (**3**)	50	2			
	70	16			
$Cp_2ZrMe(OAr)$ (**4**)	50	20		166 000	
	90		55		17 000
$Cp_2Zr(OAr)_2$ (**5**)	50	32		94 000	
	70	40			
	90	52	121	63 000	24 000
$Cp_2Zr(OAr)_2$ (**6**)	50	46		132 000	
	70	90			
	90	70	100	63 000	20 000
$Cp_2Zr(OAr)_2$ (**7**)	50	2			
	70	31			
	90		130		25000
$Cp_2ZrMe(pyr)$ (**8**)	50	4		30 000	
$Cp_2Zr(pyr)_2$ (**9**)	90	2	23	13 300	22 000
$Cp_2Zr(dff)_2$ (**11**)	90		31		16 200

[a] Kg (PE)/10^{-3} mol Zr.
[b] $[NHMe_2(C_6H_5)][B(C_6F_5)_4]$.

planar tetra-atomic ring with Zr, whereas in molecule **A** significant deviations from planarity are observed. Furthermore, the Me group deviates from the Zr–N–CH–N mean planes by 0.16(1) Å in **A**, but only −0.02(1) Å in **B**. The Me–Zr is also shorter in **A** than in **B**, with Zr–C(14) bond lengths equal to 2.314(8) and 2.341(6) Å, respectively.

It is instructive to compare the structure of $Cp_2Zr(2,6\text{-}OC_6H_3Me_2)_2$, $Cp_2Zr(2,4,6\text{-}OC_6H_2Me_3)_2$ and $Cp_2ZrMe\{CH(NC_6H_5)_2\}$ to those of other complexes of similar type such as Cp_2ZrMe_2 and $[Cp_2ZrMe]_2O$ [10]. In the formamidinato complex discussed here, the Zr–Me distances (2.314(8) and 2.341(6) Å) are comparable to those of Cp_2ZrMe_2 (2.280(5) and 2.273(5) Å) and of $[Cp_2ZrMe]_2O$ (2.276(9) Å)

Similarly, in the latter complexes the values of the X(1)–Zr–X(2) angles where X indicate the centroids of the Cp ligands, are 132.5 and 128.5° respectively; the corresponding angles in molecule **A** and **B** of the formamidinato complex have similar values 129.1(3) and 128.8(3)°.

Also comparable are the Zr–X distances which are in the range to 2.23 to 2.25 Å in the complexes. This values shows that the more crowed coordination sphere of the formamidinato complex does not affect significantly the mode of bonding of the two Cp ligands.

In both molecules **A** and **B** the two C–N bonds are almost equal in length (N(1)–C(1) 1.320(8), N(2)–C(1) 1.309(6); (N(1A)–C(1A) 1.312(6), N(2A)–C(1A) 1.321(6) and their values (1.31, 1.32 Å) correspond to a bond order of 1.5 [11], suggesting extensive electron delocalization within the tetra-atomic Zr–N–C–N ring somewhat greater for **B** than for **A**, as in the former the Zr–N–C–N ring is closer to planarity and two Zr–N bond lengths (Zr(2)–N(1A) 2.356(4) Å) and (Zr(2)–N(2A) 2.343(4) Å) are closer to one another than those of **A** (Zr(1)–N(1) 2.367(4) Å) and (Zr(1)–N(2) 2.324(4) Å). It is worthwhile to notice that the molecular structure of the analogous bis-cyclopentadienyl (cyclohexylformamidine)-Zr-chloride derivative [12] shows similar behaviour in the solid state including the presence of two molecules in the asymmetric unit with differences comparable to those of the present structures.

3. Polymerization of ethylene

The polymerization of C_2H_4 was investigated using compounds **1**–**9** and **11** as catalysts in the presence of either MAO or $[NHMe_2(C_6H_5)][B(C_6F_5)_4]$ as cocatalyst. The results are summarized in Table 3 which also lists for comparison the results obtained under comparable

Table 4
Experimental data for the crystallographic analyses

Compound	**(5)**	**(6)**	**(11)**
Formula	$ZrC_{26}H_{28}O_2$	$ZrC_{28}H_{32}O_2$	$ZrC_{24}H_{24}N_2$
Mol wt.	463.7	491.8	665.4
Color	Orange	Colorless	Yellow
Crystal size, mm	$0.32\times0.22\times0.36$	$0.32\times0.44\times0.48$	$0.26\times0.32\times0.30$
Crystal system	Orthorhombic	Monoclinic	Monoclinic
Space group	$P2_12_12_1$ (n. 19)	$P2_1/a$ (n. 14)	Pa (n. 7)
a (Å)	13.636(3)	15.291(3)	11.721(2)
b (Å)	13.932(3)	8.048(2)	11.766(2)
c (Å)	11.852(2)	40.990(6)	15.740(3)
β (°)		99.78(4)	111.02(3)
V (Å^3)	2251.6(8)	4971(2)	2026.2(7)
Z	4	8	4
$D_{calc.}$ (g cm^{-3})	1.368	1.314	1.415
$F(000)$	960	2048	888
θ range (°)	3–26	3–26	3–27
Radiation (λ, Å)	Mo–K_α(0.71073)	Mo–K_α(0.71073)	Mo–K_α(0.71073)
μ (cm^{-1})	5.06	4.63	5.52
T (K)	293	293	293
No. reflections collected	2249	8373	4803
No. observed [$I\geq3\sigma(I)$]	2184	7915	4403
No. parameters	291	571	493
$R=\Sigma\|F_o\|-\|F_c\|/\Sigma\|F_o\|$	0.052	0.054	0.033
^aR_w (on F^2)	0.124	0.133	0.084
GOF	1.20	1.21	1.31
$\Delta\rho_{max}$ (e Å^{-3})	0.77	0.52	0.29
$\Delta\rho_{min}$ (e Å^{-3}	-0.88	-0.78	-0.91

[a] $w=1/[\sigma^2(F_o^2)+(0.0397P)^2+5.04P]$ for **5**, $w=1/[\sigma^2(F_o^2)+(0.0349P)^2+10.39P]$ for **6**, $w=1/[\sigma^2(F_o^2)+(0.0339P)^2+1.22P]$ for **11**; $P=\max(F_o^2+2F_c^2)/3)$.

conditions with the well known catalysts **1** and **2**. The polymer yields obtained with the catalysts investigated in this work are in the range of those previously reported for other systems of this type [3]; yields were higher with MAO as cocatalyst than with $[NHMe_2(C_6H_5)][B(C_6F_5)_4]$. With MAO at 90°C, the aryloxide complexes gave polymer yields intermediate between those of the **1** and **2**, whereas **9** and **11** gave much lower yields. With $[NHMe_2(C_6H_5)][B(C_6F_5)_4]$, at 50, 70 and 90°C the same catalyst generally gave a monotonic increase of yields; an exception was **6**, which at 70°C produced the highest yields comparable to or even higher than those obtained with the model catalysts **1** and **2**. In contrast, yields obtained with $Cp_2Zr(pyr)_2$ remained low even at high temperature. The molecular weights of the polymers were in the range 10^4–$1.7x10^5$; in general, lower molecular weights were obtained with MAO as cocatalyst than with $[NHMe_2(C_6H_5)][B(C_6F_5)_4]$. It should be noted that the molecular weights obtained with **1** and **2** increased with temperature (from 50 to 90°C), whereas the reverse occurred with the phenoxide derivatives **5** and **6**.

The dependence of productivity on the type of aryloxide follows the trend $OC_6H_4{}^tBu > OC_6H_3Me_2 > OC_6H_3Me_3$ in presence of MAO, whereas with $[NHMe_2Ph][B(C_6F_5)_4]$ the trend is $OC_6H_2Me_3 > OC_6H_3Me_2 > OC_6H_4{}^tBu > OC_6H_5$. Thus, the electron donating properties of the OAr ligand appear to operate in opposite direction depending on the cocatalyst. Again when L = OAr, complexes containing substituted phenyl groups have greater productivity than the non-substituted analog **3**, suggesting that steric affects are negligible, at least when $[NHMe_2(C_6H_5)][B(C_6F_5)_4]$ is the cocatalyst. This relative absence of steric effects is most likely related to the easy rotation of the phenyl rings around the O–C bonds, as demonstrated by the existence of different conformations of these molecules in the solid state, which does not hamper the coordination of ethylene to the Zr atom. The Cp_2ZrL_2 complexes of monodentate ligands were generally found to be superior catalysts with respect to those of bidentate ligands (L = pyrazolyl, formamidinato), in agreement with the stronger coordination ability of bidentate ligands even though $\eta^2 \rightleftharpoons \eta^1$ equilibria can not be ruled out.

The above data indicate that different active centers are generated from the different complexes. If this occurs by interaction with MAO and $[NHMe_2(C_6H_5)][B(C_6F_5)_4]$, then the following reactions may be hypothesized:

$$Cp_2ZrL_2 + MAO \rightarrow Cp_2ZrL^+ + [L(MAO)]^-$$

$$Cp_2ZrL_2 + [NHMe_2(C_6H_5)][B(C_6F_5)_4]$$

$$\rightarrow Cp_2ZrL^+ + LH + [NMe_2(C_6H_5)] + [B(C_6F_5)_4]^-$$

Here analogy with the commonly studied systems for which the ubiquitous active cationic species is postulated $[Cp_2ZrCH_3]^+$ should suggest ethylene insertion into the Zr–O and Zr–N bonds of aryloxide, formamidinato and pyrazolide cations respectively, with formation of species of the type (a)

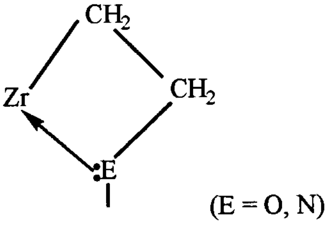

(a)

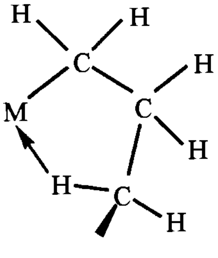

(b)

in which internal coordination acts as a stabilizing factor similarly to the agostic interaction [5] of the type shown in (b). The above scheme is unprecedented and needs more experimental support.

Table 5
Final atomic coordinates for $Cp_2Zr\{2,6\text{-}OC_6H_3(CH_3)_2\}_2$ and equivalent isotropic displacement parameters ($Å^2 \times 10^3$)

Atom	x	y	z	U(eq)
Zr	0.16261(5)	0.65998(4)	0.25646(5)	44.4(2)
O(1)	0.0418(3)	0.5789(4)	0.2579(5)	53(2)
O(2)	0.2562(4)	0.5652(4)	0.3225(4)	47(2)
C(1)	−0.0478(6)	0.5660(5)	0.3031(7)	50(3)
C(2)	−0.1315(6)	0.5964(5)	0.2484(9)	58(2)
C(3)	−0.2239(7)	0.5863(8)	0.296(1)	73(4)
C(4)	−0.2311(8)	0.5436(8)	0.401(1)	76(4)
C(5)	−0.1503(8)	0.5119(8)	0.4558(9)	64(3)
C(6)	−0.0569(7)	0.5195(6)	0.4089(7)	56(3)
C(7)	−0.1216(9)	0.6398(8)	0.1296(8)	83(4)
C(8)	0.0301(7)	0.4788(7)	0.4694(8)	69(3)
C(9)	0.3299(6)	0.5034(5)	0.3022(6)	44(2)
C(10)	0.3088(5)	0.4105(5)	0.2622(7)	50(2)
C(11)	0.3879(7)	0.3491(6)	0.2417(8)	63(3)
C(12)	0.4816(8)	0.3750(8)	0.263(1)	73(3)
C(13)	0.5004(8)	0.4646(9)	0.3019(9)	74(4)
C(14)	0.4269(7)	0.5311(6)	0.3247(7)	56(3)
C(15)	0.4477(8)	0.6256(7)	0.375(1)	89(4)
C(16)	0.2068(6)	0.3773(6)	0.244(1)	65(3)
C(17)	0.187(1)	0.7352(9)	0.4482(8)	85(5)
C(18)	0.090(1)	0.7241(9)	0.4377(9)	82(4)
C(19)	0.057(1)	0.784(1)	0.354(1)	100(6)
C(20)	0.136(2)	0.8332(8)	0.314(1)	108(8)
C(21)	0.218(1)	0.802(1)	0.371(1)	105(6)
C(22)	0.2324(9)	0.5975(8)	0.0718(7)	71(4)
C(23)	0.1417(9)	0.638(1)	0.0456(7)	84(5)
C(24)	0.148(1)	0.736(1)	0.0654(8)	94(6)
C(25)	0.241(1)	0.7568(9)	0.102(1)	93(6)
C(26)	0.2948(9)	0.6724(9)	0.1062(8)	79(4)

Table 6
Atomic coordinates for non-hydrogen atoms and equivalent isotropic thermal parameters ($Å^2 \times 10^3$) for $Cp_2ZrMe\{CH(NC_6H_5)_2\}$

Atom	x	y	z	U(eq)
Zr(1)	0.5840	0.26484(4)	0.45908(2)	41.0(1)
N(1)	0.7875(3)	0.2829(3)	0.5627(3)	45(1)
N(2)	0.6347(4)	0.3116(4)	0.6116(3)	45(1)
C(1)	0.7526(4)	0.2992(4)	0.6327(3)	45(1)
C(2)	0.5858(4)	0.3177(4)	0.6819(3)	45(1)
C(3)	0.6192(5)	0.2386(5)	0.7527(3)	55(2)
C(4)	0.5725(6)	0.2479(6)	0.8218(4)	70(2)
C(5)	0.4929(6)	0.3321(7)	0.8217(4)	80(3)
C(6)	0.4589(6)	0.4094(6)	0.7517(5)	79(2)
C(7)	0.5045(5)	0.4027(5)	0.6822(4)	62(2)
C(8)	0.9108(4)	0.2763(4)	0.5724(3)	46(2)
C(9)	1.0065(5)	0.3084(5)	0.6510(4)	58(2)
C(10)	1.1264(5)	0.3018(6)	0.6559(5)	68(2)
C(11)	1.1551(6)	0.2652(6)	0.5838(5)	71(2)
C(12)	1.0621(7)	0.2298(6)	0.5061(5)	81(3)
C(13)	0.9408(6)	0.2366(5)	0.4995(4)	66(2)
C(14)	0.3979(6)	0.2837(8)	0.4777(5)	79(3)
C(15)	0.585(1)	0.0596(6)	0.5079(6)	100(4)
C(16)	0.6827(8)	0.0687(5)	0.4805(7)	92(3)
C(17)	0.6381(9)	0.0909(6)	0.3876(6)	100(4)
C(18)	0.5112(8)	0.0947(7)	0.3577(6)	91(3)
C(19)	0.4782(8)	0.0738(7)	0.4318(7)	103(4)
C(20)	0.619(1)	0.3537(9)	0.3249(7)	118(4)
C(21)	0.4985(8)	0.3634(9)	0.3084(5)	95(3)
C(22)	0.479(1)	0.434(1)	0.3655(8)	126(5)
C(23)	0.6759(9)	0.420(1)	0.395(1)	129(6)
C(24)	0.589(2)	0.4721(7)	0.4237(7)	152(9)
Zr(2)	0.95269(5)	0.22191(3)	1.12071(2)	40.8(1)
N(1A)	0.9128(4)	0.3704(3)	1.0136(3)	44(1)
N(2A)	0.9032(5)	0.1918(3)	0.9644(3)	47(1)
C(1A)	0.8929(4)	0.3013(4)	0.9444(3)	42(1)
C(2A)	0.8961(5)	0.1132(4)	0.8947(3)	49(1)
C(3A)	0.9645(5)	0.1283(5)	0.8390(4)	61(2)
C(4A)	0.9491(6)	0.0570(6)	0.7656(5)	77(2)
C(5A)	0.8669(7)	−0.0317(5)	0.7489(4)	77(3)
C(6A)	0.8022(6)	−0.0509(5)	0.8050(5)	70(2)
C(7A)	0.8152(6)	0.0220(4)	0.8780(4)	62(2)
C(8A)	0.8761(4)	0.4851(4)	0.9984(3)	45(1)
C(9A)	0.7729(5)	0.5179(4)	0.9274(3)	53(2)
C(10A)	0.7403(6)	0.6319(5)	0.9160(4)	70(2)
C(11A)	0.8086(7)	0.7137(5)	0.9741(4)	69(2)
C(12A)	0.9098(6)	0.6816(4)	1.0442(4)	65(2)
C(13A)	0.9464(5)	0.5686(4)	1.0591(3)	53(2)
C(14A)	0.9412(9)	0.0237(5)	1.1070(5)	84(3)
C(15A)	1.1585(5)	0.3144(6)	1.1428(5)	68(2)
C(16A)	1.1344(5)	0.3294(8)	1.2223(5)	84(3)
C(17A)	1.1378(6)	0.222(1)	1.2631(5)	95(4)
C(18A)	1.1632(6)	0.1426(8)	1.2081(6)	90(3)
C(19A)	1.1746(6)	0.1983(7)	1.1340(5)	76(3)
C(20A)	0.8194(6)	0.3529(6)	1.1716(5)	81(3)
C(21A)	0.7411(6)	0.2947(8)	1.1003(5)	82(3)
C(22A)	0.7426(8)	0.1812(9)	1.1264(8)	114(4)
C(23A)	0.8276(9)	0.1739(8)	1.2160(7)	119(4)
C(24A)	0.8702(7)	0.2826(7)	1.2421(5)	81(3)

At present we would emphasize that all systems present their own peculiarities and then whatever the nature of the active species these should be related to the respective catalyst precursor. In fact it must be

Table 7
Atomic coordinates and equivalent isotropic displacement parameters (Å^2 × 10^3) for $Cp_2Zr\{2,4,6\text{-}OC_6H_2(CH_3)_3\}_2$

Atom	*x*	*y*	*z*	*U*(eq)
Zr(1)	0.08679(2)	0.67893(4)	0.36937(1)	39.5(1)
O(1)	−0.0378(2)	0.6524(3)	0.34578(8)	46(1)
O(2)	0.0731(2)	0.5932(4)	0.41373(8)	48(1)
C(1)	−0.1015(3)	0.5739(5)	0.3245(1)	42(1)
C(2)	−0.1352(3)	0.4196(5)	0.3332(1)	44(1)
C(3)	−0.2009(3)	0.3420(6)	0.3112(1)	52(2)
C(4)	−0.2351(3)	0.4111(7)	0.2805(1)	57(2)
C(5)	−0.2019(3)	0.5630(7)	0.2726(1)	59(2)
C(6)	−0.1359(3)	0.6459(6)	0.2940(1)	50(2)
C(7)	−0.1026(3)	0.3416(6)	0.3664(1)	56(2)
C(8)	−0.3059(4)	0.3203(9)	0.2563(2)	87(3)
C(9)	−0.1031(4)	0.8130(6)	0.2846(1)	69(2)
C(10)	0.0668(3)	0.6334(5)	0.4455(1)	47(1)
C(11)	−0.0124(3)	0.6978(6)	0.4531(1)	59(2)
C(12)	−0.0151(5)	0.7428(7)	0.4856(2)	78(2)
C(13)	0.0569(5)	0.7236(7)	0.5107(2)	77(2)
C(14)	0.1319(5)	0.6519(7)	0.5029(2)	76(2)
C(15)	0.1391(3)	0.6047(7)	0.4708(1)	61(2)
C(16)	−0.0939(3)	0.7132(9)	0.4275(2)	81(2)
C(17)	0.0517(7)	0.776(1)	0.5462(2)	123(4)
C(18)	0.2210(4)	0.5219(9)	0.4629(2)	91(2)
C(19)	0.0583(5)	0.9644(6)	0.3923(2)	90(3)
C(20)	0.0457(5)	0.9806(6)	0.3581(2)	89(3)
C(21)	0.1269(6)	0.9569(6)	0.3486(2)	88(3)
C(22)	0.1877(4)	0.9302(7)	0.3764(2)	80(3)
C(23)	0.1478(5)	0.9325(7)	0.4027(2)	83(3)
C(24)	0.2223(3)	0.4979(7)	0.3712(2)	73(2)
C(25)	0.1513(4)	0.3906(6)	0.3650(2)	69(2)
C(26)	0.1051(4)	0.4239(7)	0.3343(2)	75(2)
C(27)	0.1475(5)	0.5537(9)	0.3210(2)	89(3)
C(28)	0.2210(4)	0.5972(7)	0.3440(2)	92(3)
Zr(2)	0.18815(3)	0.68923(5)	0.13532(1)	49.5(2)
O(1A)	0.0806(2)	0.6522(4)	0.15598(8)	55(1)
O(2A)	0.1408(2)	0.6035(4)	0.09004(9)	60(1)
C(1A)	0.0431(3)	0.5529(5)	0.1766(1)	47(1)
C(2A)	0.0067(3)	0.3990(6)	0.1654(1)	49(2)
C(3A)	−0.0274(3)	0.2976(6)	0.1879(1)	56(2)
C(4A)	−0.0281(3)	0.3434(6)	0.2200(1)	56(2)
C(5A)	0.0049(3)	0.4996(6)	0.2300(1)	59(2)
C(6A)	0.0398(3)	0.6051(6)	0.2088(1)	54(2)
C(7A)	0.0020(3)	0.3447(6)	0.1298(1)	62(2)
C(8A)	−0.0625(4)	0.2277(8)	0.2442(2)	79(2)
C(9A)	0.0750(4)	0.7758(7)	0.2204(2)	74(2)
C(10A)	0.1076(4)	0.6412(6)	0.0581(1)	64(2)
C(11A)	0.1605(5)	0.6117(9)	0.0340(2)	88(3)
C(12A)	0.1264(7)	0.657(1)	0.0010(2)	118(4)
C(13A)	0.0435(8)	0.727(1)	−0.0077(2)	111(4)
C(14A)	−0.0082(6)	0.7458(9)	0.0161(2)	96(3)
C(15A)	0.0224(4)	0.7035(7)	0.0489(2)	74(2)
C(16A)	−0.0388(5)	0.722(1)	0.0734(2)	107(3)
C(17A)	0.0094(9)	0.775(1)	−0.0443(2)	170(6)
C(18A)	0.2483(5)	0.528(1)	0.0433(3)	147(5)
C(19A)	0.2722(6)	0.4160(9)	0.1386(2)	95(3)
C(20A)	0.2363(4)	0.4188(8)	0.1655(2)	85(3)
C(21A)	0.2708(6)	0.538(1)	0.1857(2)	97(3)
C(22A)	0.3321(5)	0.6180(9)	0.1724(3)	111(4)
C(23A)	0.3360(5)	0.550(1)	0.1412(3)	134(4)
C(24A)	0.2394(7)	0.9686(8)	0.1581(2)	101(3)
C(25A)	0.1515(6)	0.9892(7)	0.1470(2)	102(4)
C(26A)	0.1388(5)	0.9725(7)	0.1126(2)	87(3)
C(27A)	0.2208(7)	0.9468(8)	0.1040(2)	109(4)
C(28A)	0.2814(5)	0.9460(8)	0.1323(3)	112(4)

taken into account that aryloxide, amidinato and pyrazolide ligands are more strongly bounded to Zr than chloride and alkyl groups and then removal of both L ligands, especially the second one, from Zr by cocatalyst should result quite difficult.

Therefore the formation of active species of the type $[Cp_2ZrH]^+$ by hydrogenation of Zr–E (E = O, N) bonds should be considered unlikely as in our experiments the H_2 pressure is rather low, and examples are reported in literature in which Zr–O [13] and $\overline{\mathrm{M{-}N{-}C{-}N}}$ (M = Y, Sc) [14] bonds are stable also under high H_2 pressure. Moreover **3**-MAO and **6**-MAO systems have shown significant activity in copolymerization of ethylene and propylene in H_2 free atmosphere (productivity = 3, 5–6 Kg mol^{-3} Zr h^{-1}) [15].

Concerning the molecular weight distribution, several preliminary experiments of melt flow index have been carried out. The values of melt index ratio range between 20–30, thus indicating a polydispersity (M_w/M_n) between 2 and 3, a rather narrow molecular weight distribution as expected for metallocene homogeneous catalysts.

4. Conclusion

Several new O and N-bonded zirconocene complexes were synthesized in very high yields and excellent purity by a convenient one-pot reaction and the structures of four members of the series were established by X-ray crystallography. The complexes showed catalytic activity for ethylene polymerization when combined with an excess of MAO or a stoicheiometric quantity of $[NHMe_2(C_6H_5)][B(C_6F_5]_4]$. Both the catalytic activity and the molecular weight of the polymers produced were found to depend not only on the cocatalyst and on the temperature but also on the nature of the L,L^1 ligands associated to the zirconocene moieties in the Cp_2ZrLL^1 complexes. This dependence offers the opportunity for further control of the polymer properties.

5. Experimental

5.1. Materials and procedures

All operations were carried out in glove boxes under a pre-purified and controlled dinitrogen atmosphere. The hydrocarbon and ether solvents were purified by refluxing with sodium-benzophenone. Commercially available methyllithium (1.6 M solution in diethyl ether, Aldrich), $ZrCl_4$, aryloxides, pyrazole and *N*,*N′*-diphenylformamidine were used as received. Potassium cyclopentadiene was synthesized from cyclopentadiene monomer (freshly distilled) and potassium hydroxide in dimethoxyethane [16] and its concentration was determined by acidimetric titration. Unless stated otherwise, the solvent used in each synthesis was removed by evaporation under reduced pressure and the solid product was dried under vacuum; yields were quantitative. Proton NMR spectra were recorded on a Brüker AC 200 spectrometer in anhydrous C_6D_6 solution with C_6D_5H as internal standard; chemical shifts (as δ) were referenced to $SiMe_4$. Mass spectra were obtained on a VG ZAB 2F instrument operating in electron ionization (EI) mode (70 eV, 200 mA, ion source temperature 120°C).

5.2. Synthesis of complexes

Cp_2ZrCl_2 (**1**) was prepared by reaction of $ZrCl_4$ and CpK (1:2 molar ratio) in dimethoxyethane. The product was purified by sublimation a 175°C ($2 \cdot 10^{-2}$ torr).

$Cp_2Zr(Me)_2$ (**2**) was prepared by reaction of **1** with LiMe (1:2 molar ratio) in diethylether and purified by sublimation at 75°C ($2 \cdot 10^{-2}$ torr).

$Cp_2Zr(OC_6H_5)_2$ (**3**). Complex **2** (500 mg, 2 mmol) and C_6H_5OH (376 mg, 4 mmol) were dissolved in toluene (50 cm^3) and stirred for 4 h. The solvent was removed to give pure colourless $Cp_2Zr(OC_6H_5)_2$ (m.p. 130°C). ^1H NMR: 5.95 (s, 10H, Cp), 6.75–7.29 (m, 10H, OC_6H_5).

$Cp_2Zr(Me)(2,6\text{-}OC_6H_3Me_2)$ (**4**). Complex **2** (500 mg, 2 mmol) and HO-2,6-$C_6H_3Me_2$ (243 mg, 1 mmol) were stirred 2 h in toluene (50 cm^3). After removal of the solvent the pale yellow complex (m.p. 84°C) was collected. ^1H NMR: 5.68 (s, 10H, Cp), 0.49 (s, 3H, Me), 2.07 (s, 6H, 2,6-$OC_6H_3Me_2$), 6.80–7.02 (m, 3H, O-C_6H_3).

$Cp_2Zr[2,6\text{-}OC_6H_3Me_2]_2$ (**5**). Complex **2** (500 mg, 2 mmol), dissolved in toluene (50 cm^3) was treated with HO-2,6-$C_6H_3Me_2$ (486 mg, 4 mmol). After the mixture was refluxed for 10 h, the solvent was removed to give a pale yellow solid (m.p. 173°C). ^1H NMR: 5.89 (s, 10H, Cp), 2.23 (s, 12H, Me), 6.82–7.02 (m, 6H, $OC_6H_3Me_2$).

$Cp_2Zr[2,4,6\text{-}OC_6H_2Me_3]_2$ (**6**). Complex **2** (500 mg, 2 mmol) was dissolved in toluene (50 cm^3), HO-2,4,6-$C_6H_2Me_3$ (544 mg, 4 mmol) was added, and the solution was refluxed for 10 h. The solvent was removed and the pale yellow solid product was washed with *n*-hexane (10 cm^3); m.p. 139°C. ^1H NMR: 5.93 (s, 10H, Cp), 2.24 (s, 12H, *o*-CH_3), 2.26 (s, 6H, *p*-CH_3), 6.92 (s, 2H, OC_6H_2).

$Cp_2Zr(OC_6H_4)_2\text{-}4^tC_4H_9$ (**7**). Complex **2** (500 mg, 2 mmol) and HO-C_6H_6-$4^tC_4H_9$ (542 mg, 4 mmol) were refluxed for 3 h in 50 cm^3 of toluene. After drying a colourless residue was collected. ^1H NMR: 6.01 (s, 10H, Cp), 1.33 (s, 18H, $^tC_4H_9$), 6.79 and 7.32 (both doublets, 4H total, O-C_6H_4).

$Cp_2Zr(Me)(C_3H_3N_2)$ (**8**). Complex **2** (500 mg, 2 mmol) and $C_3H_4N_2$ (136 mg, 2 mmol) dissolved in 50 cm^3 of toluene, were stirred at room temperature for 2 h. After drying, the colourless solid had ^1H NMR spectrum very similar to that published recently [8]: 5.55 (s, 10H, Cp), 0.59 (s, 3H, CH_3), 6.35 (br, 1H) and 7.39 (br, 2H), both with unresolved splitting, $C_3H_3N_2$.

$Cp_2Zr(C_3H_3N_2)_2$ (**9**). Complex **1** (584 mg, 2 mmol) and $Li(C_3H_3N)$ (280 mg, 4 mmol) were suspended in 100 cm^3 of benzene and stirred at room temperature for 1 h. The mixture was centrifuged to separate insoluble LiCl; the supernatant solution was filtered and the solid residue washed with two portions of benzene (10 cm^3). The solution was evaporated to give a colourless solid. ^1H NMR: 5.75 (s, 10H, Cp), 6.24 (t, 2H, CH^b), 7.35 (d, 4H, CH^a).

$Cp_2Zr(Me)[CH(NC_6H_5)_2]$ (**10**). Complex **2** (500 mg, 2 mmol) and $(C_6H_5)NHCHN(C_6H_5)$ (391 mg, 2 mmol) were dissolved in 50 cm^3 of toluene and the mixture was stirred at room temperature for 2 h. The solvent was removed and the pale yellow solid was dried. ^1H NMR: 5.68 (s, 10H, Cp), 0.09 (s, 3H, CH_3), 7.98 (s, 1H, CH formyl), 6.71–6.80 (m, 10H, phenyl).

$Cp_2Zr[CH(NC_6H_5)_2]_2$ (**11**). Diethylether 100 cm^3, cooled to 0°C, 2.5 ml of a 1.6 molar solution of $LiCH_3$ (4 mmol) and *N*,*N′*-diphenylformamidine (785 mg, 4 mmol) were mixed and allowed to stand for 2 h. The diethyl ether was removed and 100 cm^3 of benzene containing **1** (585 mg, 2 mmol) were added. After 1 h agitation, the suspension was centrifugated. The supernatant was filtered to give a yellow residue. ^1H NMR 5.91 (s, 5H, Cp), 7.83 (s, 2H, CH), 6.67–7.14 (m, 10H, phenyl).

6. Ethene polymerization

Polymerization experiments were carried out by the following general procedure. A 3L autoclave, electrically heated and equipped with a stirring bar, was dried under dinitrogen flux at 115°C for 2 h and cooled to room temperature. The autoclave was charged with purified *n*-hexane (2L), 50–100 mg of catalyst suspended in 70 cm^3 of *n*-hexane and 30 cm^3 of toluene containing a quantity of a 10% solution of MAO (WITCO) calculated to give a 2500:1 MAO: catalyst mole ratio. At this point 14.8 bar of ethylene and 0.2 bar of H_2 were introduced, the system was heated to the polymerization temperature for 1 h. The resulting mixture was gravity filtered, the gummy polymer heated at 60°C for 2 h and weighed. Viscosity was determined in 1,2,4-trichlorobenzene solution, using a Schott Gerate Mod. AS U 360 viscosimeter thermostated at 135°C. Similar procedures were adopted when using $[NHMe_2(C_6H_5)][B(C_6F_5)_4]$ as cocatalyst. In this case 0.08 g of $Al(^iBu)_3$ were added as schavenger. Melt index of the polymer obtained with $[NHMe_2(C_6H_5)][B(C_6F_5)_4]$ has been determined for the systems **1**, **2**, **4**, **5** and **6** following the literature [17].

6.1. X-ray measurements and structure determination

Crystal data, collected reflections and parameters of the final refinement for $Cp_2Zr(2,6\text{-}OC_6H_3Me_2)_2$ (**5**), $Cp_2Zr(2,4,6\text{-}OC_6H_2Me_3)_2$ (**6**), and $Cp_2ZrMe\{CH(NC_6H_5)_2\}$ (**11**) are reported in Table 4. Reflections were collected using a Philips PW1100 diffractometer [18] with graphite-monochromated Mo–K_α radiation. The orientation matrix and cell dimensions were determined by least squares refinement of the angular positions of 30 reflections. Two standard reflections were monitored every 200 reflections and no significant decay was observed during data collection. All intensities were corrected for Lorentz polarization and absorption [19]. The positions of the heavy atoms were obtained from Patterson syntheses [20]. All non-H atoms were located in the subsequent Fourier maps. Structures were refined by full-matrix least squares using anisotropic temperature factors for all non-H atoms. Hydrogen atoms were introduced at calculated positions in their described geometries and during refinement were allowed to ride on the attached carbon atoms with fixed isotropic thermal parameters (1.2 U(eq) of the parent carbon atom). For the structures **5** and **11** the Flack parameters [21] have been refined. Calculations were performed with the SHELX-93 program [22], using the scattering factors inclosed therein. The program for the ORTEP drawing was taken from ref. [23]. Final atomic coordinates are given in Tables 5–7.

References

[1] H. Sinn, W. Kaminsky, Adv. Organometal. Chem. 18 (1980) 99.
[2] R.F. Jordan, Adv. Organometal. Chem. 32 (1991) 325.
[3] P. Möhring, N.J. Coville, J. Organometal. Chem. 479 (1994) 1.
[4] H.B. Brintzinger, D. Fischer, R. Mülhaupt, B. Rieger, R.M. Waymouth, Angew. Chem. Int. Ed. Engl. 34 (1995) 1143.
[5] M. Bochmann, J. Chem. Soc. Dalton Trans. (1996) 255.
[6] M.A. Giardello, M.S. Eisen, C.L. Stern, T.J. Marks, J. Am. Chem. Soc. 117 (1995) 12114.
[7] R. Gomez, M.L.H. Green, J.I. Haggit, J. Chem. Soc. Dalton Trans. (1996) 939. (a) These compounds were described [8, 9] when the works was in progress. P. Zanella, L. Crosara, F. Benetollo, G. Rossetto, C. Scelza, XIX Congresso Nazionale Ricerca e Tecnologia, Riccione, Italy, June 9–14, (1996), CI/CO-P2.
[8] D. Rottger, G. Erker, M. Grehl, R. Frölich, Organometallics 13 (1994) 3897.
[9] W.A. Howard, T.M. Trnka, G. Parkin, Inorg. Chem. 34 (1995) 5900.
[10] W.E. Hunter, D.C. Hrncir, R.V. Bynum, R.A. Penttila, J.L. Atwood, Organometallics 2 (1983) 750.
[11] R. Duchateau, C.T. van Wee, A. Meetsma, P.T. van Duijnen, J.H. Teuben, Organometallics 15 (1996) 2279.
[12] S. Gambarotta, S. Strologo, C. Floriani, A. Chiesi-Villa, C. Guastini, J. Am. Chem. Soc. 107 (1985) 6278.
[13] K.I. Gell, B. Posin, J. Schwartz, G. Williams, J. Am. Chem. Soc. 104 (1982) 1846.
[14] (a) C.J. Schaverien, Organometallics 13 (1994) 69. (b) J.R. Hagadorn, J. Arnold, Organometallics 15 (1996) 984.
[15] Our preliminary results.
[16] W.L. Jolly, Inorg. Synth, XI (1968) 113.
[17] D.W. Van Krevelen, Properties of Polymers, Elsevier, Amsterdam, 1990, p. 675.
[18] D. Belletti, FEBO. A New Hardware and Software System for controlling a Philips PW1100 Single Crystal Diffractometer. Internal Report 1/93. Centro di Studio per la Strutturistica Diffattometrica del CNR, Parma.
[19] A.C.T. North, D.C. Philips, F.S. Mathews, Acta Cryst. A24 (1968) 351.
[20] G.M. Sheldrick, SHELXS86, Acta Cryst. A46 (1990) 467.
[21] H.D. Flack, Acta Crystallogr. A39 (1983) 876.
[22] G M. Sheldrick, SHELXL93, Programm for the Refinement of Crystal Structures. University of Göttingen, Germany.
[23] C.K. Johnson, ORTEP II report ORNL-5138, Oak Ridge National Laboratory Tennessee, USA, 1976.